



Published in final edited form as:

J Pharm Sci. 2016 March ; 105(3): 1156–1163. doi:10.1016/S0022-3549(15)00189-6.

Investigation of the changes in aerosolization behavior between the jet-milled and spray-dried colistin powders through surface energy characterization

Teresa Jong¹, Jian Li¹, David A.V. Morton^{1,*}, Qi (Tony) Zhou^{2,*}, and Ian Larson^{1,*}

¹Drug Delivery, Dynamics & Deposition, Monash Institute of Pharmaceutical Sciences, Monash University, 381 Royal Parade, Parkville, Victoria 3052, Australia

²Department of Industrial and Physical Pharmacy, College of Pharmacy, Purdue University, 575 Stadium Mall Drive, West Lafayette, IN 47907-2091, USA

Abstract

This study aimed to investigate the surface energy factors behind improved aerosolization performance of spray-dried colistin powder formulations compared to those produced by jet-milling. Inhalable colistin powder formulations were produced by jet-milling or spray-drying (with or without L-leucine). Scanning electron micrographs showed the jet-milled particles had irregularly angular shapes, while the spray-dried particles were more spherical. Significantly higher fine particle fractions (FPFs) were measured for the spray-dried (43.8-49.6%) vs. the jet-milled formulation (28.4 %) from a Rotahaler at 60L/min; albeit the size distribution of the jet-milled powder was smaller. Surprisingly, addition of L-leucine in the spray drying feed-solution gave no significant improvement in FPF. As measured by inverse gas chromatography, spray-dried formulations had significantly ($p < 0.001$) lower dispersive, specific and total surface energy values and more uniform surface energy distributions than the jet-milled powder. Interestingly, no significant difference was measured in the specific and total surface energy values between the spray-dried formulation with or without L-leucine. Based upon our previous findings in the self-assembling behavior of colistin in aqueous solution and the surface energy data obtained here, we propose the self-assembly of colistin molecules during spray-drying, contributed significantly to the reduction of surface free energy and the superior aerosolization performance.

Keywords

dry powder inhaler; respiratory infection; antibiotics; jet milling; spray drying; surface energy; inverse gas chromatography; self-assembly; colistin

Introduction

Oral and parenteral administrations of antibiotics are common clinical practices for the treatment of respiratory infections. However, for some antibiotics, only small proportions of

*Corresponding authors: Qi (Tony) Zhou, tonyzhou@purdue.edu; Ian Larson, ian.larson@monash.edu; David A.V. Morton, david.morton@monash.edu.

drugs are present at the infection sites in airways and hence high doses are required to maintain the local drug concentration above the minimum inhibitory concentrations (MICs).¹ Such high doses via systemic routes can cause serious side effects.² For example, intravenous administration of colistin (the last-line antibiotic for many multidrug-resistant Gram-negative bacteria) can cause nephrotoxicity in up to 45% of treated patients.^{3,4}

In contrast, inhaled therapy can deliver antibiotics directly to the infection site in the respiratory tracts, such that optimal local drug concentration and prolonged action time can be achieved with a less dose and minimized systemic exposure.^{1,5,6} For example, pharmacokinetic study of nebulized CMS solution (2 million IU) in CF patients demonstrated significantly higher drug concentrations in sputum (C_{\max} 6 mg/L) for a prolonged period (e.g. 12 hours) and negligible systemic drug exposure (C_{\max} < 0.3 mg/L).⁷ Inhaled therapy via nebulization of antibiotic solution has become popular in the clinic for the treatment of respiratory infections.⁸ Compared to wet nebulization, dry powder inhalers (DPIs) are gaining increasing interest for inhaled antibiotic treatment because in general powders are more stable than the wet formulations, provide access to higher dose in a single actuation⁹ and DPIs are more convenient to carry,^{10,11} although local side effects may occur due to inhaling high-dose powders of some drugs.⁵

Jet-milling is a common industrial approach to produce inhalable drug powders.¹² However, jet-milled powders are often highly cohesive due to the high surface energy generated during the milling process.¹³ The jet-milled powder thus often possesses poor flowability, fluidization and aerosolization properties.¹⁴ As the dose of inhaled antibiotics is usually high (e.g. up to 100 mg), particle engineering approaches (e.g. spray drying), have been extensively employed with the motivation to improve aerosol performance by altering the particle morphology, bulk density and surface energy of the drug powder.^{1,15} Particles formed from spray drying can be spherical,¹⁶ porous,¹⁷ wrinkled^{16,18} and dimpled,^{19,20} each of which are proposed to be optimized for improved aerosolization performance.²¹ Excipients and spray drying parameters can be manipulated to control the particle size, morphology and surface energy.²² Aerosol performance of powders is strongly affected by the surface energy²³ as inter-particulate forces are dependent on the surface energy of the particles.²⁴ Higher surface free energy results in larger cohesion or adhesion forces.²⁵ Incorporating excipients such as amino acids into the formulation prior to spray drying was shown to improve powder dispersion.²⁶⁻²⁸ It was hypothesized that addition of L-leucine reduces the surface energy of the particle due to its surfactant-like properties, where the hydrophobic low-energy L-leucine migrates to the surface of the droplet during spray drying.²⁶

In the recent years, inverse gas chromatography (IGC) has been increasingly exploited to measure surface energy and to investigate particulate interactions of the pharmaceutical powder formulations.²⁹⁻³¹ The principle of surface energy measurement by IGC has been extensively reviewed.^{32,33} The surface energy characteristics can be determined under either the infinite or finite dilution conditions. At the infinite dilution, Henry's law is obeyed as the low probe concentration does not allow for probe-probe interaction,³⁴ thus only interacting with the highest energy sites of the sample. As infinite dilution only measures the highest energy sites of the particle surface (usually <0.1% of the total surface area), surface energy

results from this method may not be a representation of the whole particle surface.³⁵ Finite dilution involves the gradual increase in probe concentration, hence determines the surface energy distribution over a proportion of the powder.³⁶

An earlier study reported that spray drying colistin without any excipient can successfully produce an inhalable powder with FPF_{total} of >80% via an Aerolizer at 100 L/min.³⁷ However, the aerosolization performance of spray-dried colistin has not been compared with the traditional jet-milled formulation. Furthermore, the mechanisms of high aerosol performance of spray-dried colistin powders have yet been investigated. In the present study, we compared the aerosol performance of inhaled colistin powders produced by jet milling or spray drying via a low-resistance device (Rotahaler) at a moderate flow rate of 60 L/min. We also investigated the potential use of L-leucine to improve aerosolization of colistin, and notably examined the surface energy characteristics of engineered particles. Our study provides a better understanding in the relationship between surface energy and powder aerosolization of colistin DPI formulations.

Materials & Methods

Materials

Colistin sulphate was purchased from Zhejiang Shenghua Biok Biology Co., Ltd. (Hangzhou, China). Analytical grade L-leucine, trifluoroacetic acid (TEA) and high performance liquid chromatography (HPLC) grade dichloromethane were purchased from Sigma-Aldrich (Castle Hill, Australia). HPLC grade acetonitrile (Fisher Scientific, Fair Lawn, NJ, USA), absolute ethanol (Merck, AR grade, Australia) and Milli-Q grade water (Millipore Corporation, Billerica, MA, USA) were also used in the study. GC grade undecane, decane, nonane, octane, heptanes and ethyl acetate were purchased from Fluka Aldrich (Castle Hill, Australia). Methane 5.0, helium 5.0 (both from Linde, North Ryde, Australia), compressed instrument air and hydrogen (Coregas, Yennora, Australia) gas were used. The Rotahaler was provided by GSK (Middlesex, UK). Gelatin capsules were donated by Capsugel (Peapack, USA).

Spray drying

The feed solutions were prepared with 2% w/v of colistin sulphate in MilliQ water. Various amounts of L-leucine (5, 10 and 20% w/w) were added into the feed solution prior to spray drying for those L-leucine containing formulations. The spray drying (Büchi 190 Mini Spray Dryer, Switzerland) conditions were set as: 2 mL/min pump speed; $100 \pm 5^\circ\text{C}$ inlet temperature; spray flow rate, 600 L/h; and aspirator setting, 100%. The outlet temperature remained steady at $60 \pm 5^\circ\text{C}$.

Jet milling

A spiral jet mill (model 50AS, Hosokawa Alpine, Augsburg, Germany) was employed to micronize the colistin powder. Colistin powder was fed manually into the feed chute, where it came into contact with 4 nozzles (0.8 mm diameter). An inlet air pressure of 5 bar and a grinding pressure of 6 bar were used.

Particle size distribution

A Mastersizer S (Malvern Instruments, Malvern, UK) coupled with a 300-mm Fourier lens, was used to measure the particle size distribution of colistin powder formulations. A 150 mL liquid dispersing unit was filled with ethanol and used to disperse colistin particles. The spray-dried formulations were added until an obscuration between 10% and 25% was achieved.

Scanning electron microscopy

Each powder formulation was placed onto a scanning electron microscope (SEM) mount and was coated for 3 min by an Emitech, K550X Sputter coater (Quorum Technologies Ltd, East Sussex, UK) to form a thin layer of gold with 20 nm thickness. SEM images were taken under a Phenom scanning electron microscope (FEI Company, Hillsboro, Oregon, USA).

In-vitro aerosol deposition

In-vitro aerosol deposition of the DPI formulations was assessed using a twin stage impinger (TSI) (Apparatus A, British Pharmacopoeia 2005, Copley Scientific, Nottingham, UK). While the TSI provides only a single cut with limited aerosol quality information, it was selected as considered suitable for this study to prevent particle bounce for high dose powder aerosols that may be experienced with current impactors. Stage 1 (S1) and Stage 2 (S2) were filled with 7 mL and 30 mL of water, respectively. An airflow of 60 L/min was drawn through the TSI by a Dynavac pump (Model OD5/2, Dynavac Engineering, Australia) for 4 seconds to pass 2.4 L air through the Rotahaler device. Hard gelatin capsules (Size 3, Capsugel, Sydney, Australia) were filled manually with 15 mg of powder and loaded into the Rotahaler. All TSI measurements were performed in five replicates. Recovered dose was defined as the total amount of drug collected in the Inhaler, S1 and S2. The recovery was calculated using Equation 1. Fine particle fraction (FPF) was calculated using Equation 2.

$$\% Recovery = \frac{R + S1 + S2}{Drug\ in\ capsule} \times 100 \quad \text{Equation 1}$$

$$\% FPF = \frac{S2}{R + S1 + S2} \times 100 \quad \text{Equation 2}$$

Quantification of colistin

The drug particles collected from TSI were analysed using a validated HPLC assay. A reversed-phase PhenoSphere-NEXT column (C₁₈, 5 µm, 150 mm × 4.6 mm, Phenomenex, Lane Cove, Australia) coupled with a C₁₈ guard column (5 µm, 4.0 × 3.0 mm, Phenomenex) was used. The UV wavelength was set at 210 nm on the Shimadzu diode array detector (SPD-MIOA VP, Shimadzu, Kyoto, Japan). The mobile phase comprised of 83% 35 mM triethylamine at pH 2.5 and 17% acetonitrile.³⁸ The triethylamine solution was filtered using a 0.45 µm membrane prior to acetonitrile addition. The isocratic flow rate was set at 1 mL/min and the temperature of the column oven was 25°C. Samples (30 µL) were injected and a Shimadzu Integrator (C-R5A Chromatopack) was used for peak integration. The

standard curve was linear over the concentration range of 7.8 - 250 $\mu\text{g/mL}$ ($r^2 > 0.999$). Accuracy and precision were determined using 6 replicates of quality control (QC) samples at low and high concentrations. For high QC samples (30 $\mu\text{g/mL}$), an accuracy of 29 ± 0.2 $\mu\text{g/mL}$ and a precision of 6.3% were obtained. The accuracy and precision for the low QC samples were 19.4 ± 1.1 $\mu\text{g/mL}$ and 5.9%, respectively.

Inverse gas chromatography

IGC (Surface Measurement Systems Ltd., London, UK) was used to determine the surface energy of the powders at both infinite and finite dilution conditions using the established methods.³⁰ A pre-silanized standard glass column with an internal diameter of 4 mm and a length of 300 mm was filled with the powder and consolidated with a jolting volumeter (Surface Measurement Systems Ltd., London, UK) for 5 minutes, until no cracks and further consolidation in the powder were found. For reproducibility, two separate columns were filled with the powder and each column was ran three times. The column was conditioned for 3 hours at 0% RH prior to each measurement. A conditioning time of 3 hours was experimentally determined as sufficient to reach equilibrium, since increasing conditioning time up to 15 hours resulted in no significant change in the dispersive surface energy.

At the infinite dilution condition, the probe concentration was $0.03p/p^0$ (where p denotes the partial pressure and p^0 the vapour pressure). The temperature was kept at 303 K and the flow rate of the carrier gas, helium was 10 mL/min. The gas probes used to calculate dispersive surface energy (γ_s^D) were GC grade undecane, decane, nonane, octane and heptane. Dichloromethane (basic probe) and ethyl acetate (acidic probe) were used to calculate specific free energy (G^P)³⁰. The retention time was detected with a flame ionization detector and the dead volume was measured by methane. The results were calculated by the IGC standard analysis software v1.3 (SMS, London, UK) to determine the dispersive and specific free adsorption. Using this approach, the dispersive energy was expressed in mJ/m^2 , and the specific free adsorption is expressed in Kcal/mole. The basic (γ^-) and acidic (γ^+) components of the surface were used to calculate the γ_s^P from the specific free energy adsorptions values of dichloromethane and ethyl acetate, respectively, employing the van Oss concept.^{39,40}

The G^P interactions with both dichloromethane and ethyl acetate were calculated using the Schultz approach.⁴¹ From G^P , polar surface energies (γ_s^P) were calculated using Equation 3, based on the theory of Good van Oss.^{42,43}

$$\Delta G^P = N_A \cdot a \cdot 2 \sqrt{(\gamma_L^+ \cdot \gamma_s^-) + (\gamma_L^- \cdot \gamma_s^+)} \quad \text{Equation 3}$$

Where γ_s^+ and γ_s^- are the acidic and basic parameters of the solid surface, respectively and γ_L^+ and γ_L^- are the acidic and basic parameter of the probe molecules, respectively. Where N_A is Avogadro constant and a , is the cross sectional area of the adsorbate. The polar surface energy (γ_s^P) was calculated using the γ_s^+ and γ_s^- values (Equation 4).^{42,43}

$$\gamma_s^P = S \sqrt{\gamma_s^+ \cdot \gamma_s^-} \quad \text{Equation 4}$$

Once the dispersive and polar surface energy were determined, the total surface energy (γ_s^T) was calculated by adding the dispersive and polar contributions:⁴⁴

$$\gamma_s^T = \gamma_s^D + \gamma_s^P \quad \text{Equation 5}$$

The finite dilution measurements were performed according to a literature method.³⁰ In short, all probes (decane, nonane, octane, heptanes, hexane, dichloromethane and ethyl acetate) were run at concentrations of 0.03, 0.10, 0.25, 0.55, 0.70, 0.80, 0.90 and 0.95 p/p⁰ to construct adsorption isotherms.³⁹ Dispersive surface energy distribution profiles were determined.^{31,45} The Brunauer-Emmet Teller (BET) surface area was calculated from the hexane adsorption isotherms. The surface coverage (n/n_m) for each probe at different vapor pressures was calculated from the monolayer capacity (n_m) and the adsorbed amount (n). The surface coverage can also be expressed as a percentage of surface coverage ($n/n_m \times 100$). A plot of net retention volume against surface coverage was plotted to determine the overlapping regions of surface coverage for each probe. The dispersive surface energy of the adsorbent was calculated from the gradient ($2N_A \sqrt{\gamma_s^D}$) of a plot of $RT \ln V_N$ against $a \sqrt{\gamma_L^S}$ of the alkanes, at each surface coverage. The constructed isotherm graphs were used to determine the specific free energy of adsorption (G^P) at each surface coverage using the Schultz approach.⁴¹ The specific surface energy at each surface coverage was determined from the specific free energy of adsorption based on the Good Van Oss theory.^{42,43} The total surface energy was calculated from the addition of dispersive and specific surface energy. The surface energy profiles were determined in triplicate for each powder formulation.

Statistical analysis

SPSS (Version 15.0, IBM, Armonk, New York, USA) was used for statistical analysis. Formulations were compared using one-way ANOVA analysis with a Post Hoc Tukey Test. A statistical difference was observed if p was less than 0.05.

Results & Discussion

Particle size

Particle size distributions of the jet-milled and spray-dried colistin formulations from laser diffraction are shown in Fig. 1. D_{50} values of all formulations were smaller than 5 μm . The jet-milled formulation had slightly smaller D_{50} and no significant differences in the particle size distribution were measured among all spray-dried formulations ($p > 0.05$).

Particle morphology

Representative SEM images of all formulations are presented in Fig. 2. The supplied colistin particles exhibited irregularly angular shape (Fig. 2A). After jet milling, the particle size decreased but the shape remained unchanged (Fig. 2B). In contrast, spray-dried formulations consisted of spherical or near-spherical particles with corrugated surfaces and hollow

particles with smooth surfaces (Fig. 2C-F). It is well known that such wrinkled particles form from spray drying film-forming materials such as peptides, enzymes and other natural polymers. These are proposed to form when the liquid at the surface of the droplet evaporates in the hot air from spray drying and a coherent rubbery shell forms.²² As drying proceeds, internal pressure first increases causing expansion and then decreases, contributing to the collapse of particles and forming wrinkled particles.²² Cenospheres appear as particles with holes formed in the shell; these were proposed to form as shell failure due to high internal pressures. Internal pressure was released prior to expansion and thus particles do not collapse. From the SEM images, all spray-dried particles had physical sizes smaller than 5 μm , which is in agreement with those measured by laser diffraction. Moreover, the morphology of all spray-dried formulations appeared similar regardless of presence of L-leucine.

Aerosolization performance

The jet-milled colistin powder had a relatively low FPF of $28.4 \pm 6.7\%$ (Fig. 3). After spray drying without any excipient (SDC), the FPF increased significantly to $43.8 \pm 4.6\%$ ($p < 0.05$). Notably, there was no significant difference in FPF between the spray-dried alone formulation and those spray-dried with L-leucine ($p > 0.05$).

The jet-milled particles had a smaller size distribution but inferior aerosol performance because jet-milling generally generates high free-energy surfaces during the violent collisions causing indiscriminate particle breakage. Moreover, corrugated surface produced by spray drying may also reduce cohesion of the powder by decreasing contact area.¹⁶ Therefore, particle engineering by spray drying is preferred to produce free-flowing powders of high-dose antibiotics with high aerosolization performance.¹ A growing number of research groups have demonstrated that surface modification to particles can improve aerosolization of dry powder formulations.^{22,26} The mechanism by which L-leucine increases aerosolization performance of spray-dried powders is proposed due to its surfactant-like properties and the enrichment of low-energy L-leucine on the particle surface.^{26,46} The relatively more hydrophobic alkyl side chain of the L-leucine molecule gives spray-dried colistin hydrophobic properties with a low surface energy.⁴⁷ During the drying process, L-leucine molecules are proposed to self-assemble with specific orientation of the molecules at the surface where hydrophobic tails face outwards while the hydrophilic heads face inside the droplet. As a result of the presence of hydrophobic portion of the L-leucine molecules at the outmost particle surface, the particle surface exhibits a lower surface energy which aids dispersion. On the other hand, the corrugated surface of spray-dried colistin particles may also contribute to the reduction in powder cohesion and improvement in aerosolization.

It is interesting to note that there was no significant difference ($p > 0.05$) in the FPF when colistin was spray dried with or without L-leucine. This high aerosolization efficiency of the spray-dried colistin without L-leucine is therefore proposed to be due to surface self-assembly of the colistin itself (hydrophobic tail towards the particle exterior) and hence lower surface energy. This hypothesis is supported by the findings from a study conducted

by Wallace et al.⁴⁸ that colistin exhibited such self-assembly behavior in the aqueous solution.

In this study, we propose further that the self-assembly of colistin is occurring not only in the aqueous feed solution but also during the spray drying process, allowing for specific orientation of the colistin molecule at the surface of the droplet and hence the dry particle. Consequently, the cyclic polypeptide would act as the hydrophilic head facing inwards; the fatty acyl tail with low surface energy would act as the hydrophobic tail and face outwards from the drying droplet (Fig. 4). IGC surface energy measurements were performed to confirm the low surface energy of the spray dried colistin powders.

Surface energy by IGC

Infinite dilution method—The dispersive surface energy, specific surface energy and total free surface energy of colistin formulations measured by the IGC infinite dilution method are shown in Fig. 5 - 7. The dispersive surface energy of the jet-milled formulation was 41.25 ± 1.67 mJ/m² and a reduction of 17% was measured after spray drying alone ($p < 0.05$). There was no significant difference in the dispersive surface energy among all the spray-dried powders regardless of addition of L-leucine ($p > 0.05$). The lower dispersive surface energy of all the spray-dried formulations indirectly support the proposed arrangement of colistin and L-leucine molecules during the drying process, providing self-assembled hydrophobic fatty chains oriented to the surface.

Similar to the dispersive energy data, the milled powder had significantly higher specific and total free surface energy values compared to the spray-dried formulations ($p < 0.001$). There was no significant difference in specific and total free surface energy among all the spray-dried formulations ($p > 0.05$). Fig. 8 illustrated the relationship between the total surface energy and dispersion, as the total surface energy decreased while the dispersion increased. Our study also showed that addition of L-leucine did not improve the aerosolization of the spray-dried colistin powder, as it provided no further reduction in surface energy.

The limitation of the infinite dilution method is that only the highest energy sites of the particle surface is measured and the heterogeneity of the particle surface is not considered.²⁹ Given that surface heterogeneity often presents in pharmaceutical powders,⁴⁹ IGC measurements under the finite dilution conditions were also conducted aiming to fully understand the surface energy properties of produced colistin powder formulations.

Finite dilution method—The dispersive, specific and total free surface energy data of jet-milled and spray-dried colistin samples measured by the IGC finite dilution method are shown in Figures 9 - 11, respectively. The jet-milled formulation had the highest dispersive, specific and total free surface energy values over the coverage range of finite dilution measurements ($p < 0.05$). The spray-dried formulations exhibited slightly lower dispersive energy values than that of the spray-dried alone formulation. There was no significant difference in the specific and total free surface energy values ($p > 0.05$).

The finite dilution IGC measurements provide the surface energy distribution over a range of surface coverage of a powder. It has been reported that jet milling generally leads to an increase in surface energy and heterogeneity due to the exposure of newly created high surface-energy sites.³¹ Such heterogeneity in specific and total free surface energy for the jet-milled colistin powder was evident in the present study with a significant decrease in specific and total free surface energy values when surface coverage increases (Fig. 10 and 11).

In contrast, the spray-dried formulations exhibited not only significantly lower dispersive, specific and total free surface energy values, but also more uniform distributions of surface energetic characteristics. This observation indicates that more uniform particle surface with lower surface energy was created through spray drying. The significantly reduced surface energy after spray drying is believed to be attributable to the self-assembly behavior of colistin.⁴⁸ During the spray drying process, the colistin molecules migrate to the surface of the droplet with arrangement of non-polar tails on the outside of the droplet, thereby resulting in a lower IGC measured surface energy. Such self-assembly behavior of colistin is similar to the drying behavior of L-leucine;²⁶ hence, no significant difference was detected when L-leucine was added in spray drying of colistin. Future studies in direct measurement of binding sites between colistin molecules in the spray-dried formulation (i.e. using infrared spectroscopy) are warranted to further confirm the unique self-assembly behavior of colistin.

Conclusions

This study provided fundamental investigations on the effects of spray drying on the surface energy and the aerosolization efficiency of colistin powder formulations. The spray-dried colistin formulations had substantially superior aerosol performance compared to the jet-milled powders. Surprisingly, the present study demonstrated that co-spray drying colistin with a recognized aerosolization-enhancer, L-leucine, did not change either the particle morphology or the dispersibility of the colistin formulation. The self-assembly behavior of colistin was proposed to contribute to these interesting findings in aerosolization of the colistin powders. The data from the IGC infinite and finite dilution measurements supported that: (1) specific (polar) and total surface energy of spray-dried colistin particles were markedly lower than those of jet-milled particles; (2) addition of L-leucine in the spray drying of colistin did not result in lower surface energy. Additionally, surface energy measurements by the finite dilution method showed the spray-dried colistin formulations have more uniform surface energy distributions than the jet-milled powders, supporting a more uniform surface. Further studies are warranted to directly measure the dynamics of self-assembly behavior of colistin during the drying process.

Acknowledgments

Teresa Jong acknowledges the scholarship support provided by Faculty of Pharmacy and Pharmaceutical Sciences, Monash University. Jian Li is an NHMRC Senior Research Fellow and is funded by grants from the National Institute of Allergy and Infectious Diseases of the National Institutes of Health (R01 AI098771 and AI111965). The content is solely the responsibility of the authors and does not necessarily represent the official views of the National Institute of Allergy and Infectious Diseases or the National Institutes of Health. The authors would like to thank GSK for providing inhaler devices and Capsugel for providing gelatine capsules.

References

1. Zhou QT, Leung SSY, Tang P, Parumasivam T, Loh ZH, Chan HK. Inhaled formulations and pulmonary drug delivery systems for respiratory infections. *Advanced Drug Delivery Reviews*. 2015; 85:83–99. [PubMed: 25451137]
2. Li J, Nation RL, Turnidge JD, Milne RW, Coulthard K, Rayner CR, Paterson DL. Colistin: the re-emerging antibiotic for multidrug-resistant Gram-negative bacterial infections. *The Lancet Infectious Diseases*. 6(9):589–601. [PubMed: 16931410]
3. Hartzell JD, Neff R, Ake J, Howard R, Olson S, Paolino K, Vishnepolsky M, Weintrob A, Wortmann G. Nephrotoxicity Associated with Intravenous Colistin (Colistimethate Sodium) Treatment at a Tertiary Care Medical Center. *Clinical Infectious Diseases*. 2009; 48(12):1724–1728. [PubMed: 19438394]
4. Bergen PJ, Landersdorfer CB, Zhang J, Zhao M, Lee HJ, Nation RL, Li J. Pharmacokinetics and pharmacodynamics of ‘old’ polymyxins: what is new? *Diagnostic Microbiology and Infectious Disease*. 2012; 74(3):213–223. [PubMed: 22959816]
5. Velkov T, Rahim NA, Zhou QT, Chan HK, Li J. Inhaled anti-infective chemotherapy for respiratory tract infections: Successes, challenges and the road ahead. *Advanced Drug Delivery Reviews*. 2015; 85:65–82. [PubMed: 25446140]
6. Garcia-Contreras L, Yadav KS. Inhaled formulation design for the treatment of lung infections. *Current Pharmaceutical Design*. 2015; 21(27):3875–3901. [PubMed: 26290199]
7. W S Yapa S, Li J, Patel K, Wilson JW, Dooley MJ, George J, Clark D, Poole S, Williams E, Porter CJH, Nation RL, McIntosh MP. Pulmonary and Systemic Pharmacokinetics of Inhaled and Intravenous Colistin Methanesulfonate in Cystic Fibrosis Patients: Targeting Advantage of Inhalational Administration. *Antimicrobial Agents and Chemotherapy*. 2014; 58(5):2570–2579. [PubMed: 24550334]
8. Antoniu SA, Cojocaru I. Inhaled colistin for lower respiratory tract infections. *Expert Opinion on Drug Delivery*. 2012; 9(3):333–342. [PubMed: 22332963]
9. Cipolla D, Gonda I, Chan HK. Liposomal formulations for inhalation. *Therapeutic delivery*. 2013; 4(8):1047–1072. [PubMed: 23919478]
10. Zhou Q, Tang P, Leung SSY, Chan JGY, Chan HK. Emerging inhalation aerosol devices and strategies: Where are we headed? *Advanced Drug Delivery Reviews*. 2014; 75:3–17. [PubMed: 24732364]
11. Muralidharan P, Hayes D Jr, Mansour HM. Dry Powder Inhalers in COPD, Lung Inflammation, and Pulmonary Infections. *Expert Opinion on Drug Delivery*. 2015; 12(6):947–962. [PubMed: 25388926]
12. Lin YW, Wong J, Qu L, Chan HK, Zhou QT. Powder production and particle engineering for dry powder inhaler formulations. *Current Pharmaceutical Design*. 2015; 21(27):3902–3916. [PubMed: 26290193]
13. Zhou QT, Morton DA. Drug–lactose binding aspects in adhesive mixtures: controlling performance in dry powder inhaler formulations by altering lactose carrier surfaces. *Advanced drug delivery reviews*. 2012; 64(3):275–284. [PubMed: 21782866]
14. Zhou QT, Armstrong B, Larson I, Stewart PJ, Morton DAV. Understanding the influence of powder flowability, fluidization and de-agglomeration characteristics on the aerosolization of pharmaceutical model powders. *European Journal of Pharmaceutical Sciences*. 2010; 40(5):412–421. [PubMed: 20433919]
15. Li X, Vogt FG, Hayes D Jr, Mansour HM. Physicochemical characterization and aerosol dispersion performance of organic solution advanced spray-dried microparticulate/nanoparticulate antibiotic dry powders of tobramycin and azithromycin for pulmonary inhalation aerosol delivery. *European Journal of Pharmaceutical Sciences*. 2014; 52:191–205. [PubMed: 24215736]
16. Chew NY, Tang P, Chan HK, Raper JA. How much particle surface corrugation is sufficient to improve aerosol performance of powders? *Pharmaceutical Research*. 2005; 22(1):148–152. [PubMed: 15771241]

17. Geller DE, Weers J, Heurding S. Development of an Inhaled Dry-Powder Formulation of Tobramycin Using PulmoSphere (TM) Technology. *Journal of Aerosol Medicine and Pulmonary Drug Delivery*. 2011; 24(4):175–182. [PubMed: 21395432]
18. Zhou QT, Gengenbach T, Denman JA, Heidi HY, Li J, Chan HK. Synergistic antibiotic combination powders of colistin and rifampicin provide high aerosolization efficiency and moisture protection. *The AAPS journal*. 2014; 16(1):37–47. [PubMed: 24129586]
19. Vehring R, Foss WR, Lechuga-Ballesteros D. Particle formation in spray drying. *Journal of Aerosol Science*. 2007; 38:728–746.
20. Master, K. *Spray drying handbook* ed. New York: John Wiley & sons Inc; 1991.
21. You Y, Zhao M, Lui G, Tang X. Physical characteristics and aerosolization performance of insulin dry powders for inhalation prepared by a spray drying method. *Journal of Pharmacy and Pharmacology*. 2007; 59:927–934. [PubMed: 17637186]
22. Vehring R. Pharmaceutical Particle Engineering via Spray Drying. *Pharmaceutical Research*. 2008; 25(5):999–1022. [PubMed: 18040761]
23. Grimsey IM, Feeley JC, York P. Analysis of the Surface Energy of Pharmaceutical Powders by Inverse Gas Chromatography. *Journal of Pharmaceutical Sciences*. 2002; 91(2):571–583. [PubMed: 11835214]
24. Feeley JC, York P, Sumbly BS, Dicks H. Processing effects on the surface properties of α -lactose monohydrate assessed by inverse gas chromatography (IGC). *Journal of Materials Science*. 2002; 37:217–222.
25. Li K, Sun J, Lui L, Qi Z. The influence of the surface chemical conditions on the adhesive behaviour between two transition metals. *Physica Status Solidi (a)*. 1992; 129:161.
26. Sou T, Orlando L, McIntosh MP, Kaminskas LM, Morton DAV. Investigating the interactions of amino acid components on a mannitol-based spray-dried powder formulation for pulmonary delivery: A design of experiment approach. *International Journal of Pharmaceutics*. 2011; 421:220–229. [PubMed: 21963471]
27. Vehring R, Foss WR, Lechuga-Ballesteros D. Particle formation in spray drying. *Journal of Aerosol Science*. 2007; 38(7):728–746.
28. Lechuga-Ballesteros D, Charan C, Stults CL, Stevenson CL, Miller DP, Vehring R, Tep V, Kuo MC. Trileucine improves aerosol performance and stability of spray-dried powders for inhalation. *Journal of Pharmaceutical Sciences*. 2008; 97(1):287–302. [PubMed: 17823950]
29. Zhou QT, Denman JA, Gengenbach T, Das S, Qu L, Zhang H, Larson I, Stewart PJ, Morton DAV. Characterization of the surface properties of a model pharmaceutical fine powder modified with a pharmaceutical lubricant to improve flow via a mechanical dry coating approach. *Journal of Pharmaceutical Sciences*. 2011; 100(8):3421–3430. [PubMed: 21455980]
30. Das SC, Zhou Q, Morton DAV, Larson I, Stewart PJ. Use of surface energy distributions by inverse gas chromatography to understand mechanofusion processing and functionality of lactose coated with magnesium stearate. *European Journal of Pharmaceutical Sciences*. 2011; 43(4):325–333. [PubMed: 21621612]
31. Thielmann F, Burnett DJ, Heng JYY. Determination of the surface energy distributions of different processed lactose. *Drug Development and Industrial Pharmacy*. 2007; 33:1240–1253. [PubMed: 18058321]
32. Buckton G, Gill H. The importance of surface energetics of powders for drug delivery and the establishment of inverse gas chromatography. *Advanced Drug Delivery Reviews*. 2007; 59(14): 1474–1479. [PubMed: 17928094]
33. Jones MD, Young P, Traini D. The use of inverse gas chromatography for the study of lactose and pharmaceutical materials used in dry powder inhalers. *Advanced Drug Delivery Reviews*. 2012; 64(3):285–293. [PubMed: 22265843]
34. Planinsek O, Zadnik J, Rozman S, Kunaver M, Dreu R, Srcic S. Influence of inverse gas chromatography measurement conditions on surface energy parameters of lactose monohydrate. *International Journal of Pharmaceutics*. 2003; 256:17–23. [PubMed: 12695007]
35. Ylä-Mäihänen PP, Heng JY, Thielmann F, Williams DR. Inverse gas chromatographic method for measuring the dispersive surface energy distribution for particulates. *Langmuir*. 2008; 24(17): 9551–9557. [PubMed: 18680326]

36. Thielmann F, Burnett DJ, Heng JY. Determination of the surface energy distributions of different processed lactose. *Drug Development and Industrial Pharmacy*. 2007; 33(11):1240–1253. [PubMed: 18058321]
37. Zhou Q, Morton D, Yu HH, Jacob J, Wang JP, Li J, Chan HK. Colistin powders with high aerosolisation efficiency for respiratory infection: preparation and in vitro evaluation. *Journal of Pharmaceutical Sciences*. 2013; 102(10):3736–3747. [PubMed: 23904207]
38. Cao G, Ali FEA, Chiu F, Zavascki AP, Nation RL, Li J. Development and validation of a reversed-phase high-performance liquid chromatography assay for polymyxin B in human plasma. *Journal of Antimicrobial Chemotherapy*. 2008; 62(5):1009–1014. [PubMed: 18765414]
39. Thielmann F, Pearse D. Determination of surface heterogeneity profiles on graphite by finite concentration inverse gas chromatography. *Journal of Chromatography A*. 2002; 969:323–327. [PubMed: 12385402]
40. Traini D, Young PM, Thielmann F, Acharya M. The influence of lactose pseudopolymorphic form on salbutamol sulfate–lactose interactions in DPI formulations. *Drug Development and Industrial Pharmacy*. 2008; 34:992–1001. [PubMed: 18800259]
41. Schultz J, Lavielle L, Martin C. The Role of the Interface in Carbon Fibre-Epoxy Composites. *Journal of Adhesion*. 1987; 23:45–60.
42. van Oss CJ. Acid-base interfacial interactions in aqueous media. *Colloids and Surfaces A: Physicochemical and Engineering Aspects*. 1993; 78:1–49.
43. van Oss CJ, Good RJ, Chaudhury MK. Additive and Nonadditive Surface Tension Components and the Interpretation of Contact Angles. *Langmuir*. 1988; 4:844–891.
44. Fowkes FM. Attractive Forces at Interfaces. *Industrial and Engineering Chemistry*. 1964; 56:40–52.
45. Yla-Maihaniemi PP, Heng JYY, Thielmann F, Williams DR. Inverse gas chromatographic method for measuring the dispersive surface energy distribution for particulates. *Langmuir*. 2008; 24(17):9551–9557. [PubMed: 18680326]
46. Gliniski J, Chavepeyer JK. Surface properties of aqueous solutions of L-leucine. *Biophysical Chemistry*. 2000; 84:99–103. [PubMed: 10796026]
47. Rabbani NR, Seville PC. The influence of formulation components on the aerosolisation properties of spray-dried powders. *Journal of Controlled Release*. 2005; 110(1):130–140. [PubMed: 16226334]
48. Wallace SJ, Li J, Nation RL, Prankerd RJ, Velkov T, Boyd BJ. Self-Assembly Behavior of Colistin and Its Prodrug Colistin Methanesulfonate: Implications for Solution Stability and Solubilization. *Journal of Physical Chemistry B*. 2010; 114:4836–4840.
49. Ho R, Muresan AS, Hebbink GA, Heng JY. Influence of fines on the surface energy heterogeneity of lactose for pulmonary drug delivery. *International Journal of Pharmaceutics*. 2010; 388(1):88–94. [PubMed: 20038447]

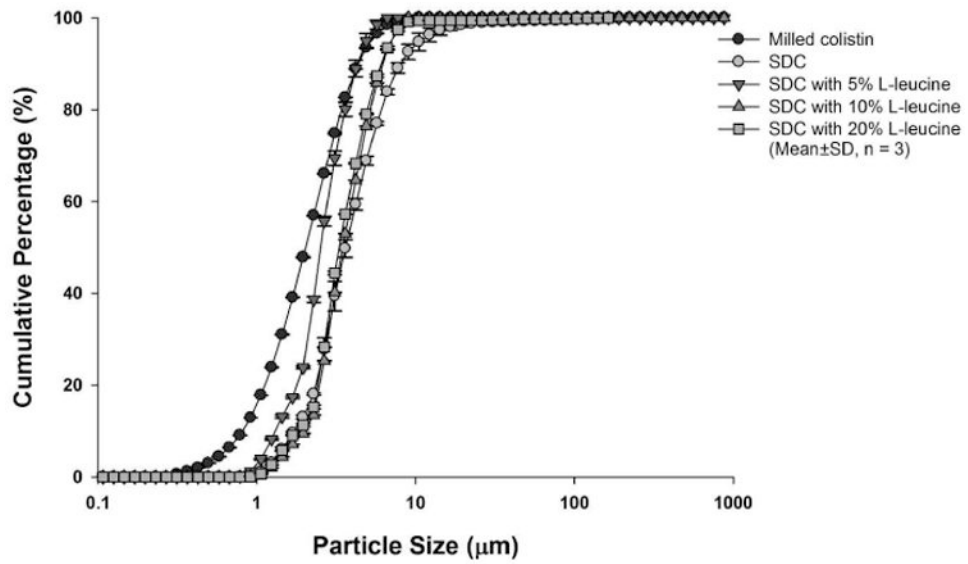


Fig 1. Particle size distributions of the milled and spray-dried (SDC) colistin formulations.

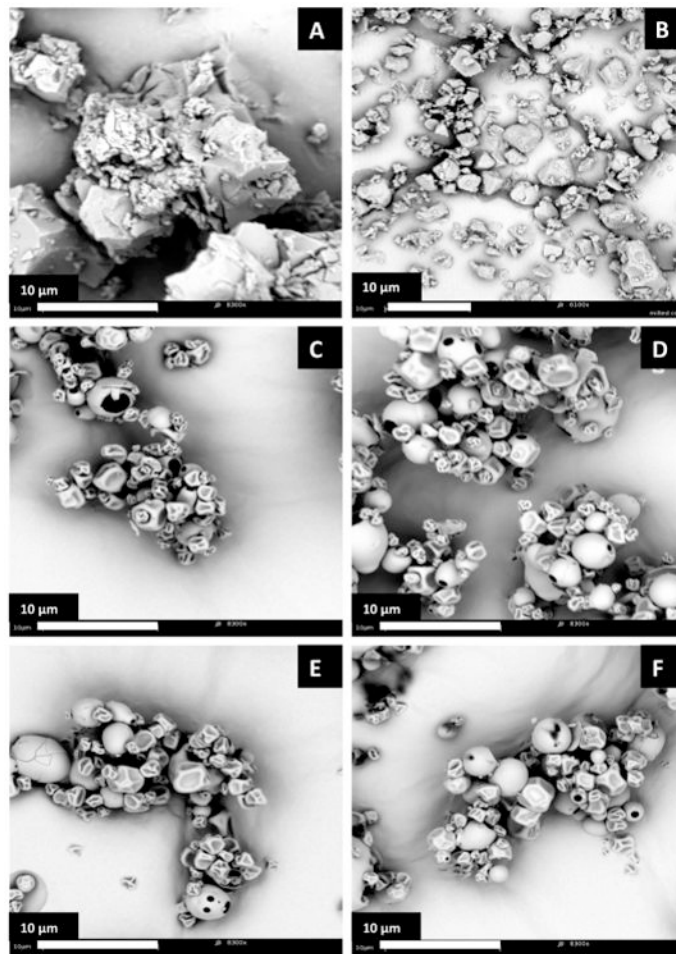


Fig. 2. SEM images of (a) supplied colistin, (b) jet-milled colistin, (c) spray-dried colistin alone, (d) spray-dried colistin with 5% w/w L-leucine, and (e) spray-dried colistin with 10% w/w L-leucine, and (f) spray-dried colistin with 20% w/w L-leucine.

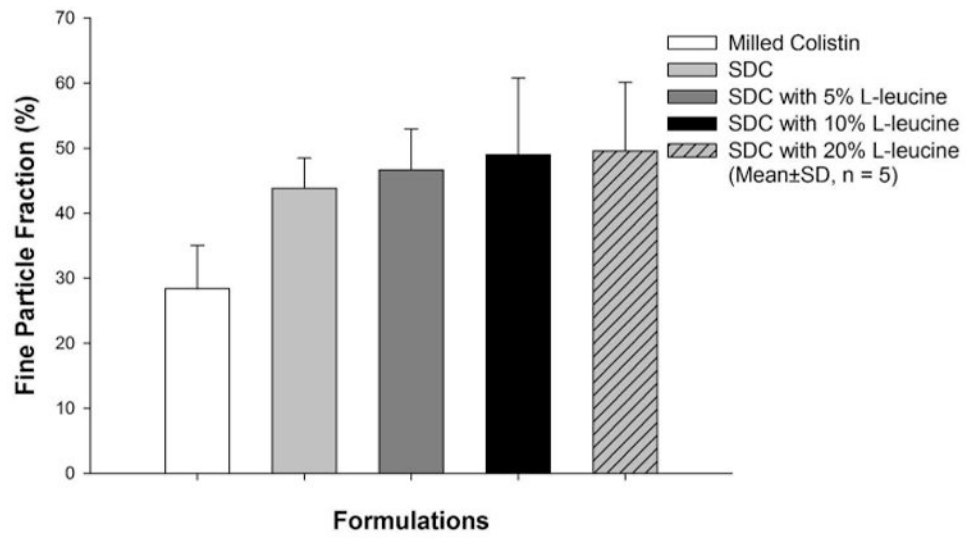


Fig. 3. FPF of jet-milled and spray-dried colistin (SDC) formulations from a Rotahaler with an airflow of 60 L/min.

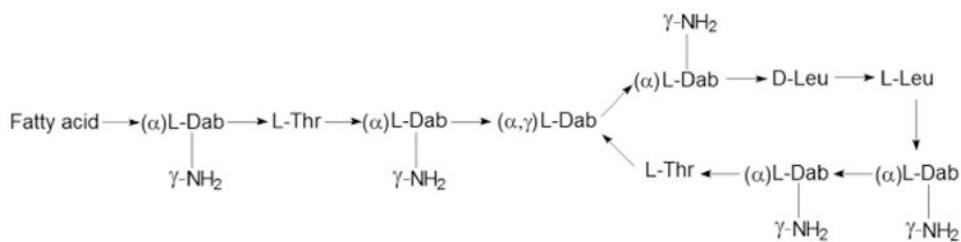


Fig. 4. Chemical structure of colistin. Fatty acid: 6-methyloctanoic acid for colistin A and 6-methylheptanoic acid for colistin B; Thr=threonine; Leu=leucine; Dab=α,γ-diaminobutyric acid. α and γ indicate the respective amino group involved in the peptide linkage. Reprinted from the literature ² with permission from Elsevier.

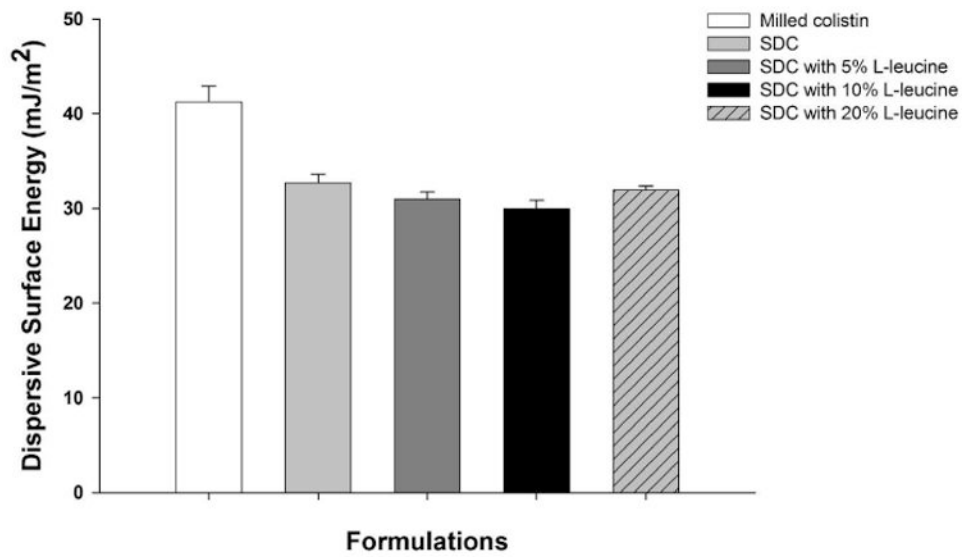


Fig. 5. Dispersive surface energy results measured by IGC under the infinite dilution condition for the colistin formulations (Mean \pm SD, n=3).

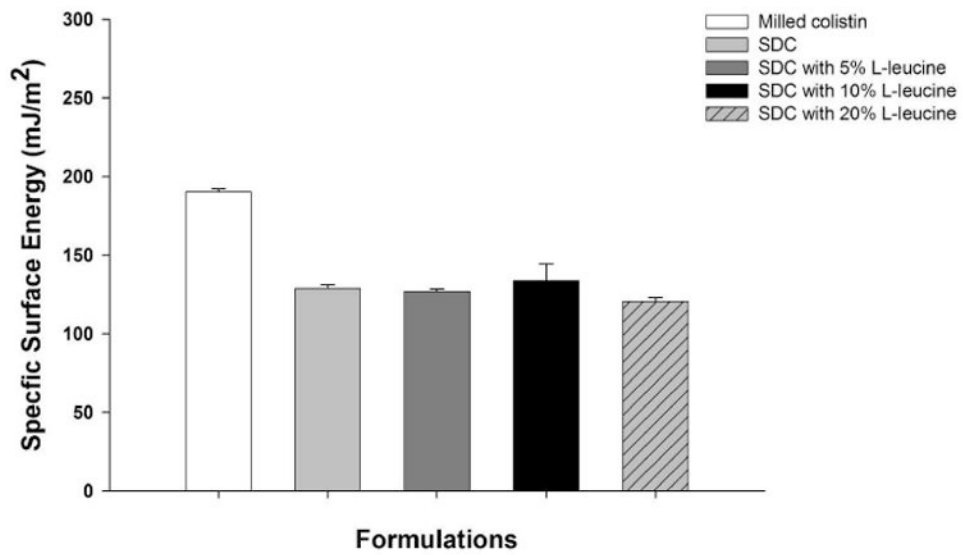


Fig. 6. Specific surface energy results measured by IGC under the infinite dilution condition for the colistin formulations (Mean \pm SD, n=3).

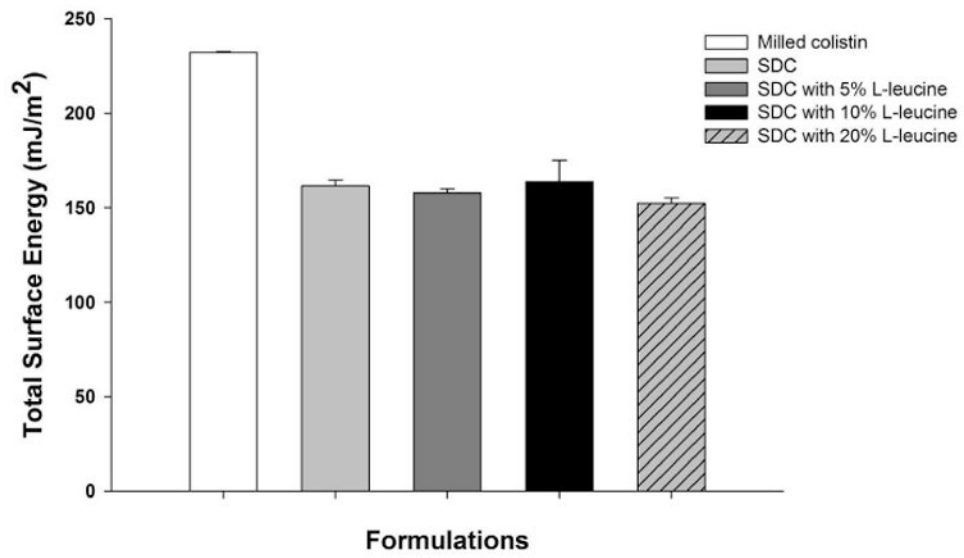


Fig. 7. Total surface energy results measured by IGC under the infinite dilution condition for the colistin formulations (Mean \pm SD, n=3).

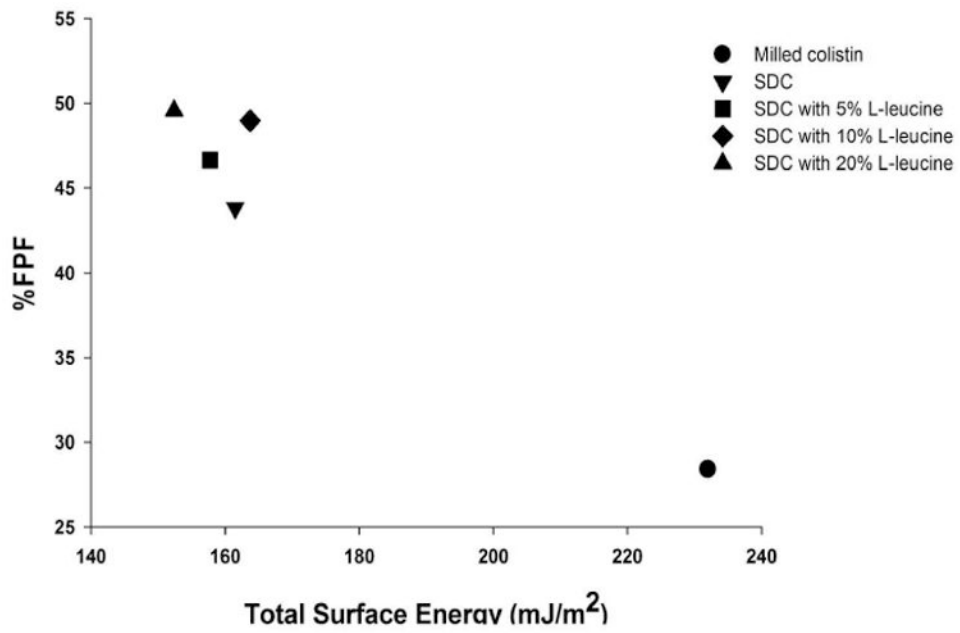


Fig. 8. Total surface energy versus FPF of the colistin formulations (Surface energy was measured by IGC under the infinite dilution condition).

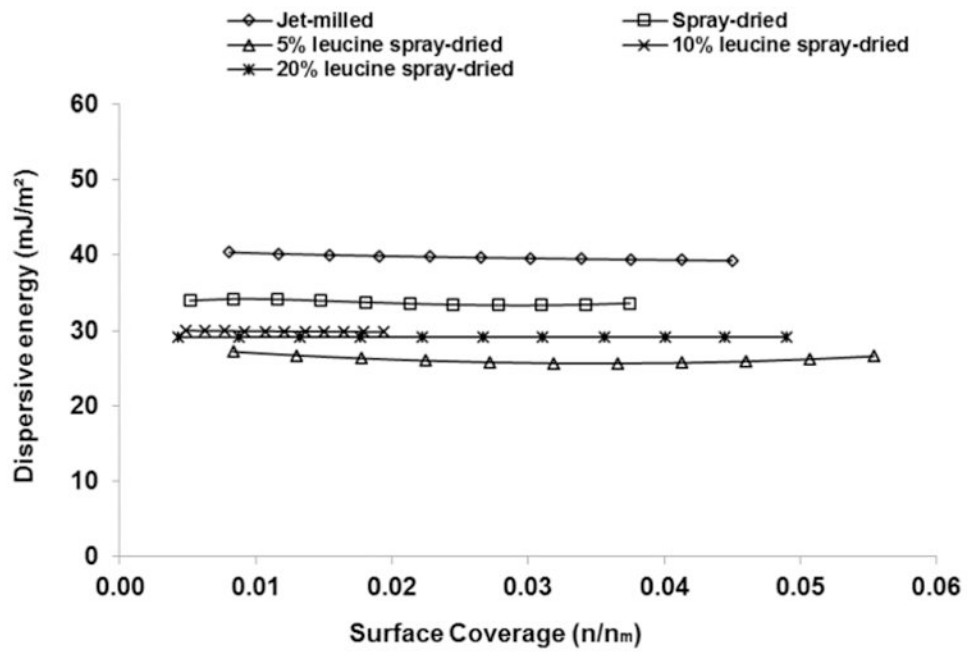


Fig. 9. Dispersive surface energy distributions measured by IGC under the finite dilution condition for the colistin formulations (Mean \pm SD, n=3).

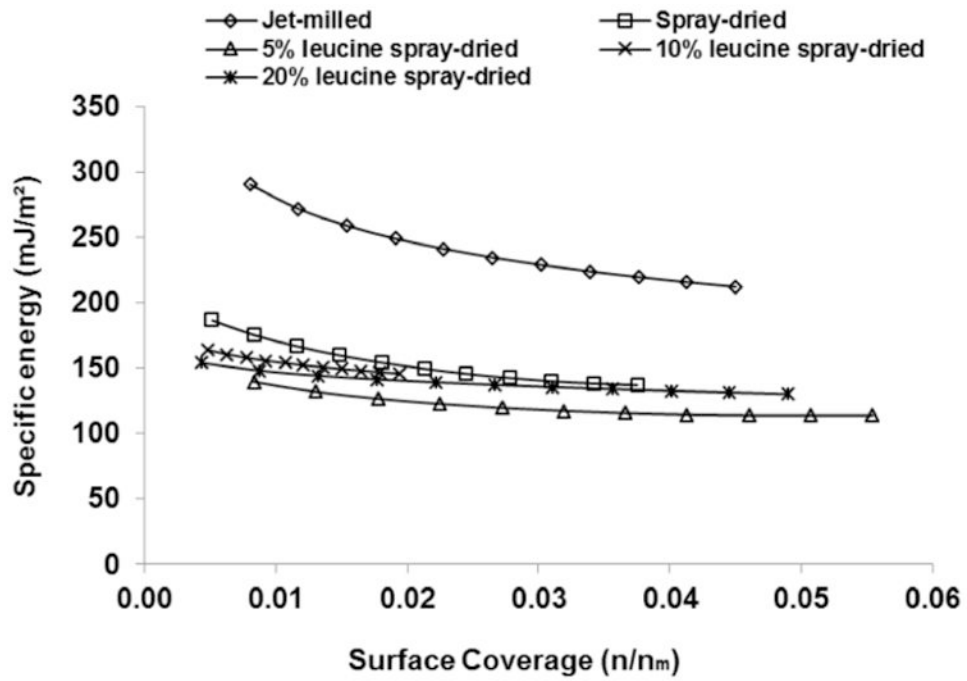


Fig. 10. Specific surface energy distributions measured by IGC under the finite dilution condition for the colistin formulations (Mean \pm SD, n=3).

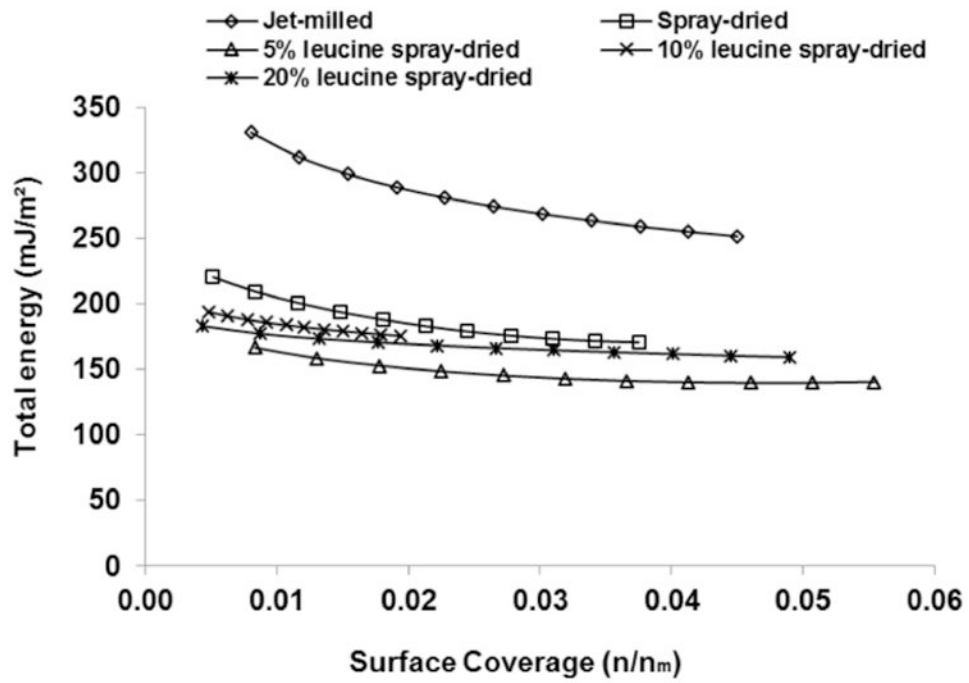


Fig. 11. Total surface energy distributions measured by IGC under the finite dilution condition for the colistin formulations (Mean \pm SD, n=3).